

MedComNet 2024

11 - 13 JUNE 2024 / NIZZA FRANCE

The Rumble in the Millimeter Wave Jungle: Obstructions Vs RIS

Juan Marcos Ramírez, Vincenzo Mancuso, Marco Ajmone Marsan

Postdoctoral Researcher

IMDEA Networks Institute

[Developing the
Science of Networks]

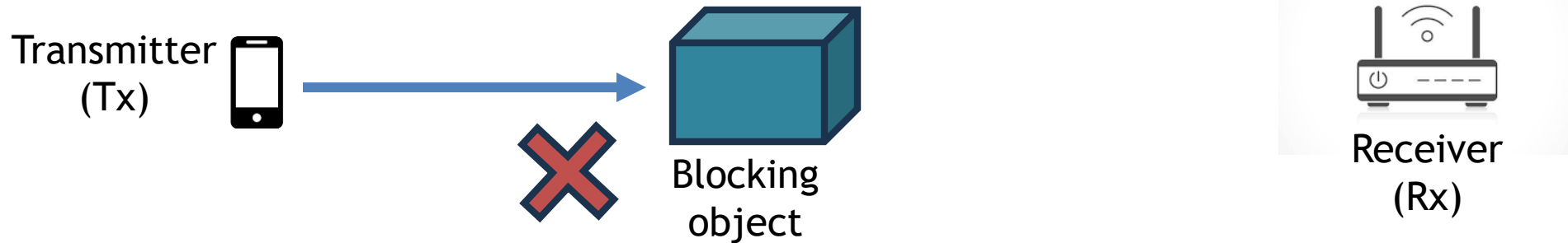
- Background and Motivation
- Reconfigurable Intelligent Surfaces
- Path Loss Model
- Probability of Outage
- Numerical Simulations
 - 2D Indoor Case
 - Beamsteering Cases
 - 3D Indoor Case
- Conclusions and Future Work

Background and Motivation



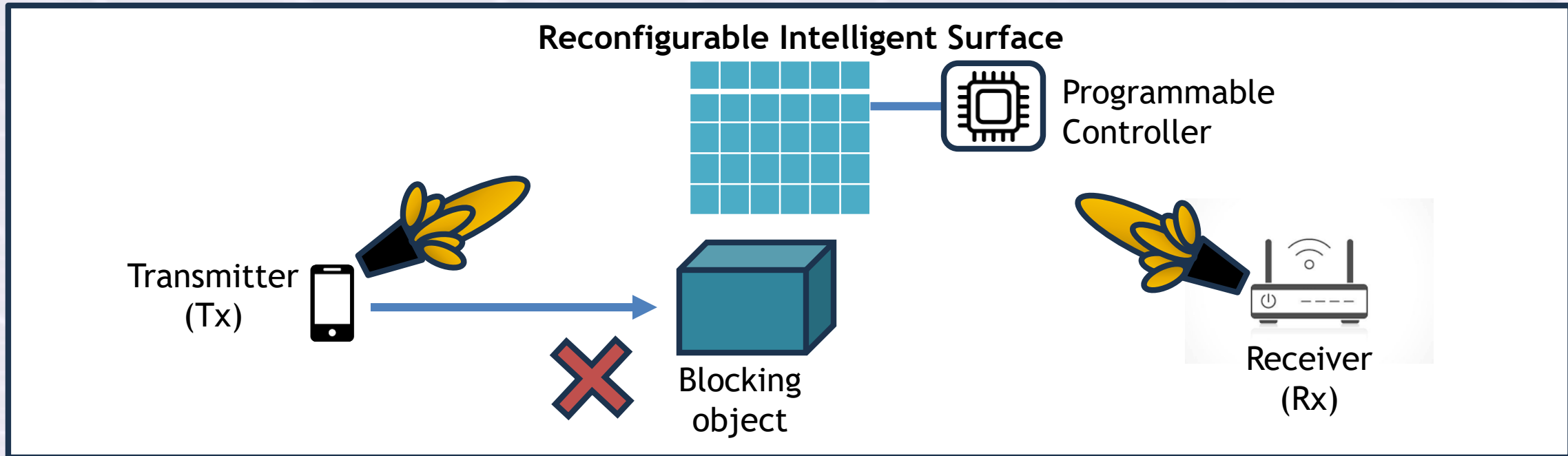
- **Sub-6 GHz Congestion:** The rapid growth in traffic is causing congestion problems in sub-6 GHz frequency bands.
- **mmWave and THz frequency bands:**
 - Provide abundant spectrum and high data transfer rates for supporting 6G technology.

Challenge: Any object can block the link path



- **Sub-6 GHz Congestion:** The rapid growth in traffic is causing congestion problems in sub-6 GHz frequency bands.
- **mmWave and THz frequency bands:**
 - Provide abundant spectrum and high data transfer rates for supporting 6G technology.
 - **Exhibit large path losses, especially when the LOS path is blocked by obstacles.**

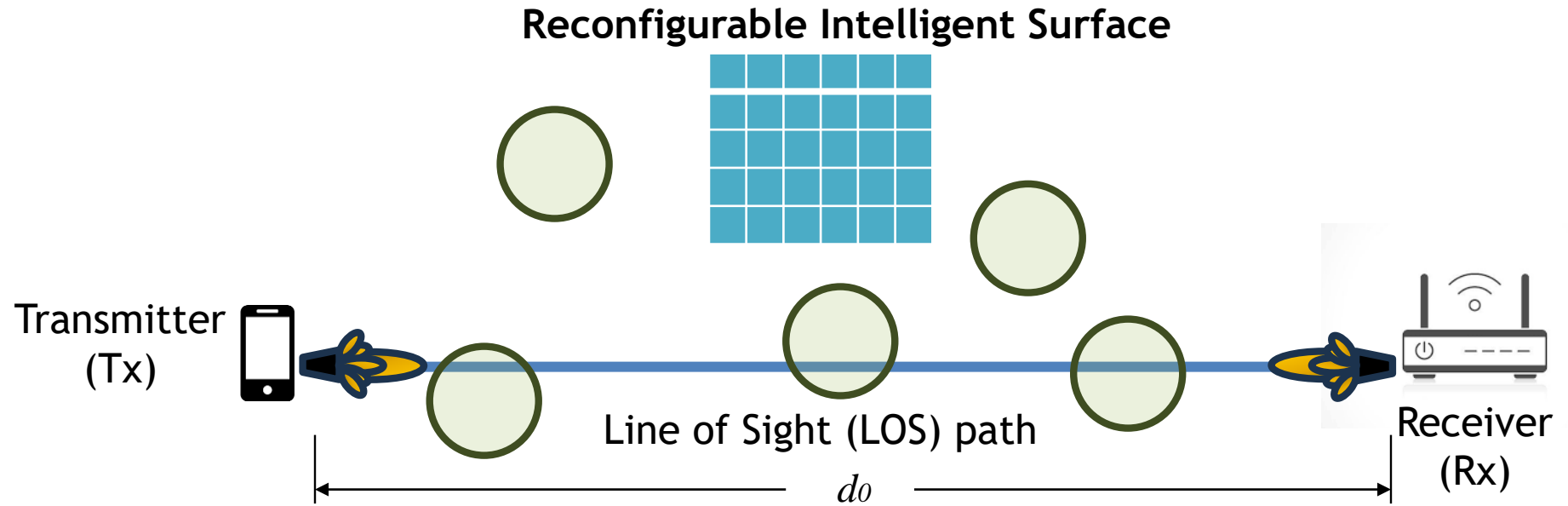
A Solution: Reconfigurable Intelligent Surfaces (RIS)



- **Essential Supporting Technology:** for 6G wireless communications
- **RIS:** are (2D) arrays of reflecting elements, allowing phase and magnitude responses to be manipulated via a programmable controller.
- **Smart Radio Environments:** RIS can provide control on wireless environment.

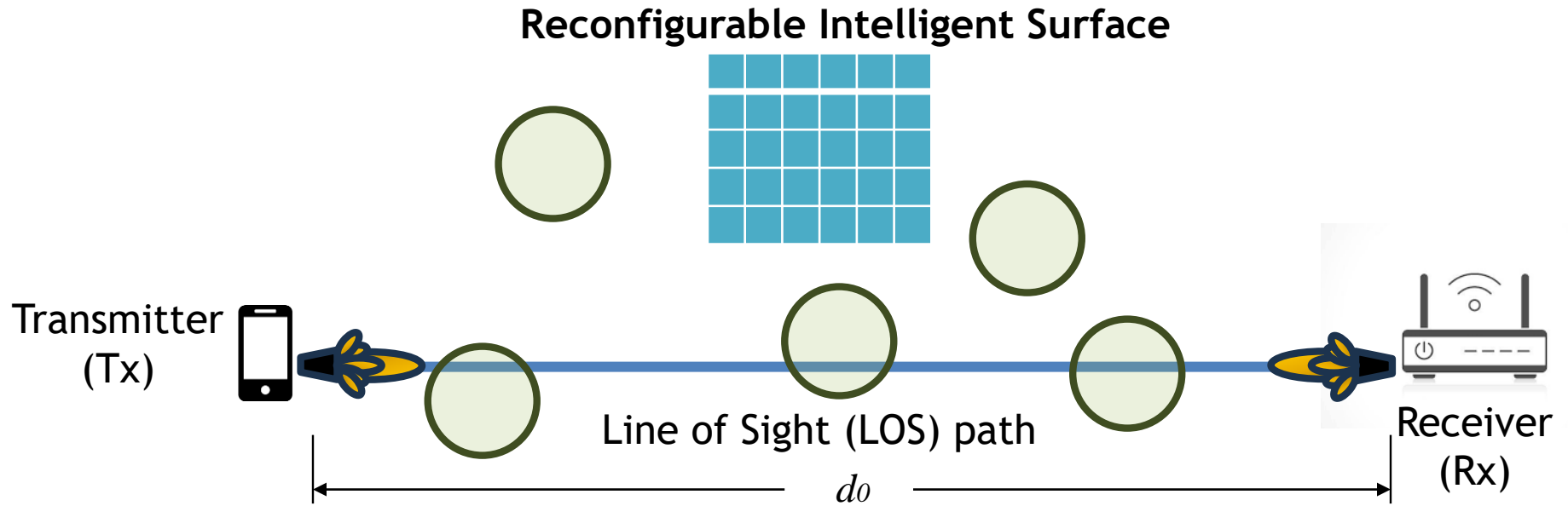
- **Path Loss Modeling:** a crucial research area for enhancing RIS-assisted wireless communication systems.
- Introduction of various path loss models [1-7].
- **Limitations of Current Models:**
 - Exclude the transmission medium effects.
 - Discard the attenuation induced by obstructing objects.
- **Importance of Comprehensive Path Loss Models:**
 - Signal-to-Noise Ratio (SNR) Calculation.
 - Outage Probability Estimation: to evaluate reliability and performance of the link in the presence of obstructions.

Line of Sight (LOS) Path Loss Modeling



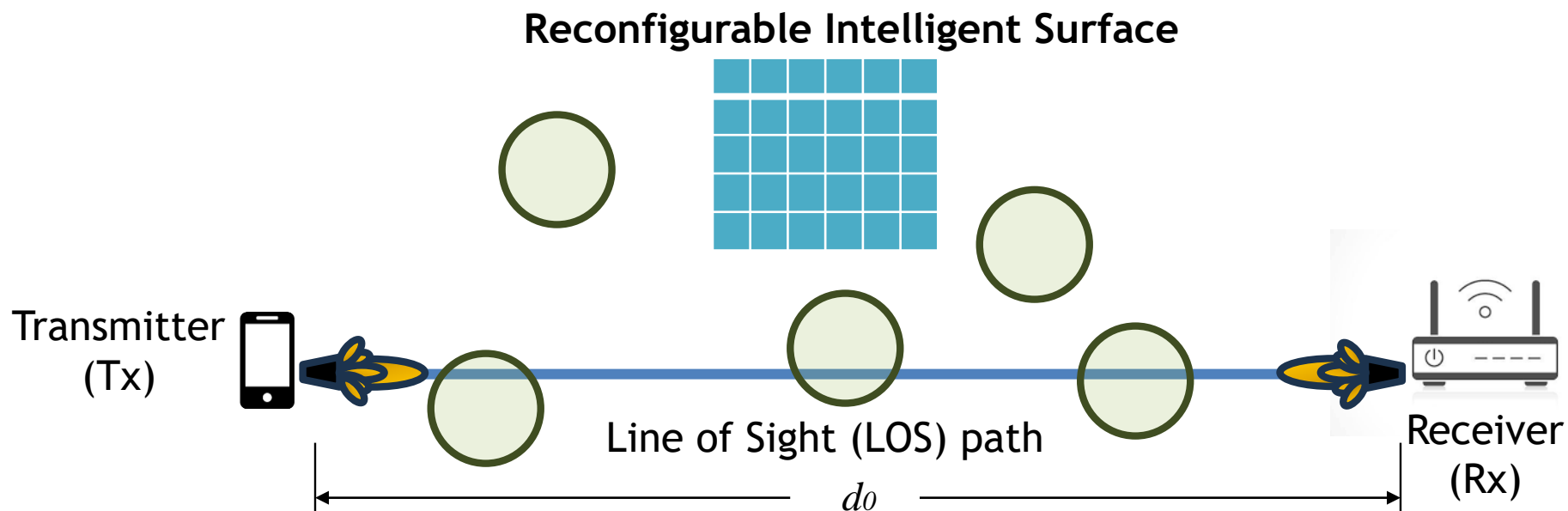
Line of Sight Path Loss Model in dB [8] $\longrightarrow \mathcal{L}_0 = L_0 + 10 \log_{10} \mu_0 + \zeta X_0, \quad (1)$

Line of Sight (LOS) Path Loss Modeling



Line of Sight Path Loss Model in dB $\longrightarrow \mathcal{L}_0 = \underbrace{L_0}_{\text{Free-Space Path Loss}} + 10 \log_{10} \mu_0 + \zeta X_0, \quad (1)$

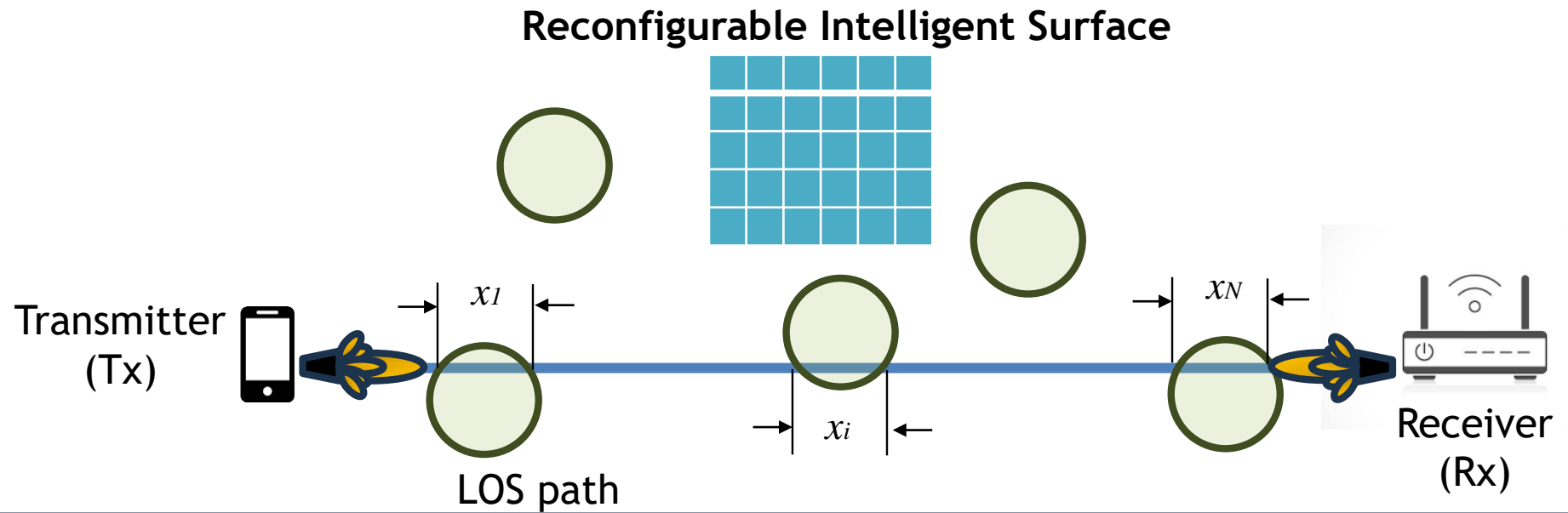
Line of Sight (LOS) Path Loss Modeling



Line of Sight Path Loss Model in dB $\longrightarrow \mathcal{L}_0 = L_0 + 10 \log_{10} \mu_0 + \zeta X_0, \quad (1)$

Term related to the average fading depth

Line of Sight (LOS) Path Loss Modeling

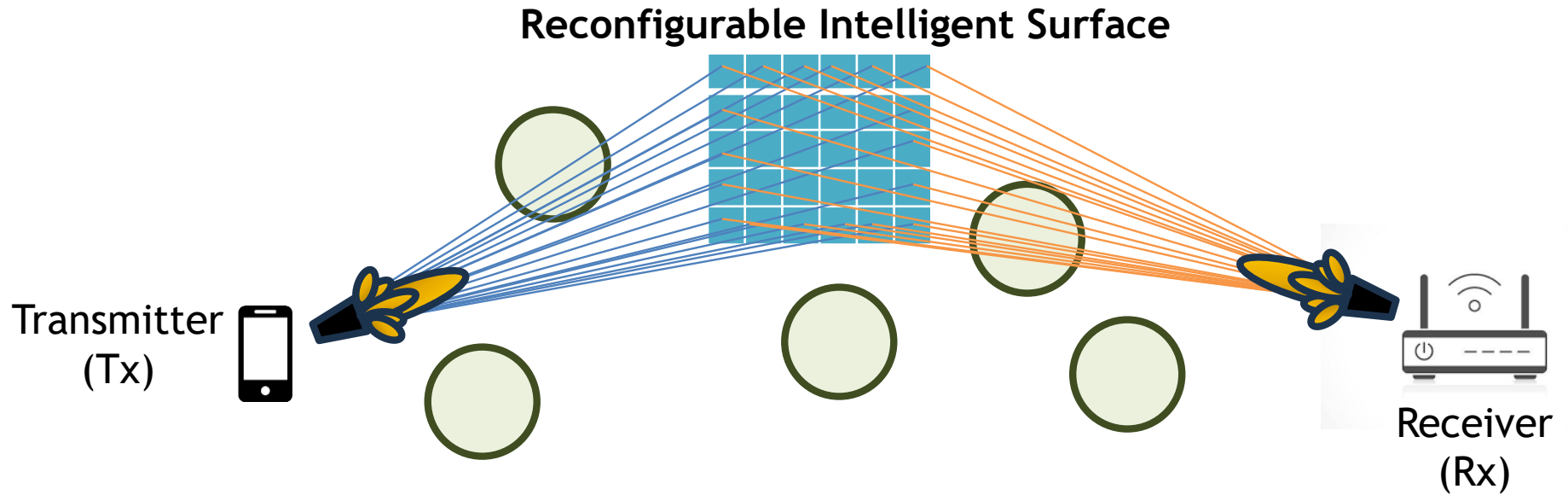


Line of Sight Path Loss Model in dB $\longrightarrow \mathcal{L}_0 = L_0 + 10 \log_{10} \mu_0 + \zeta X_0, \quad (1)$

Obstruction attenuation

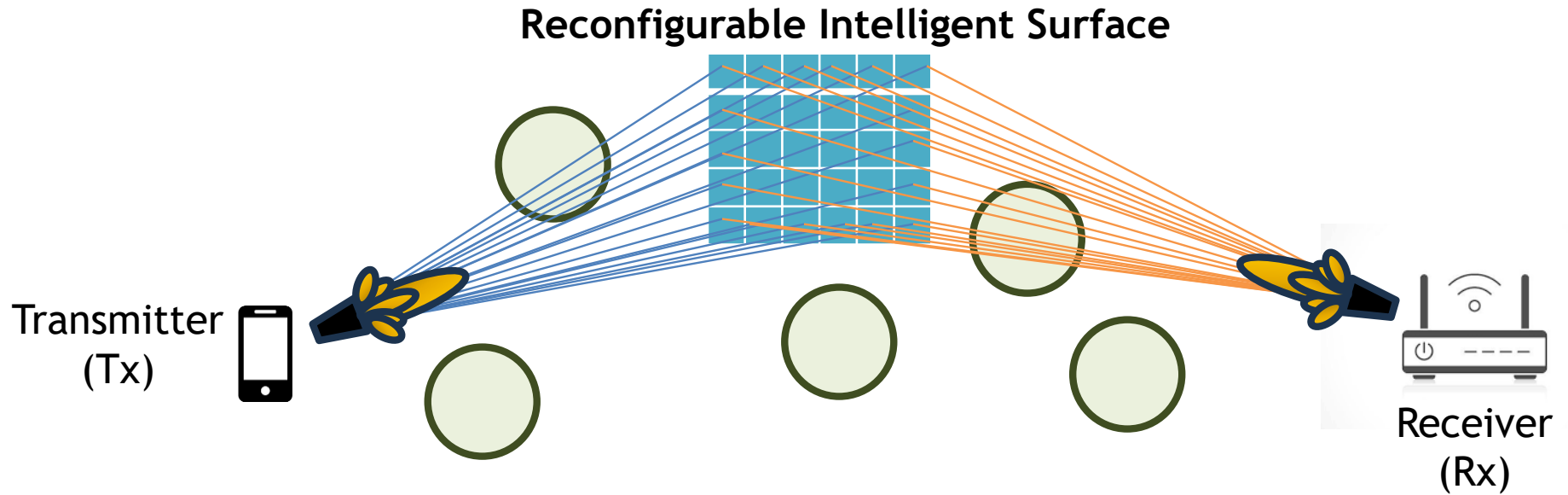
- ζ - Attenuation of the obstructing object in dB/m
- X_0 - Total obstruction length for the LOS path

$$X_0 = \sum_{i=1}^N x_i$$



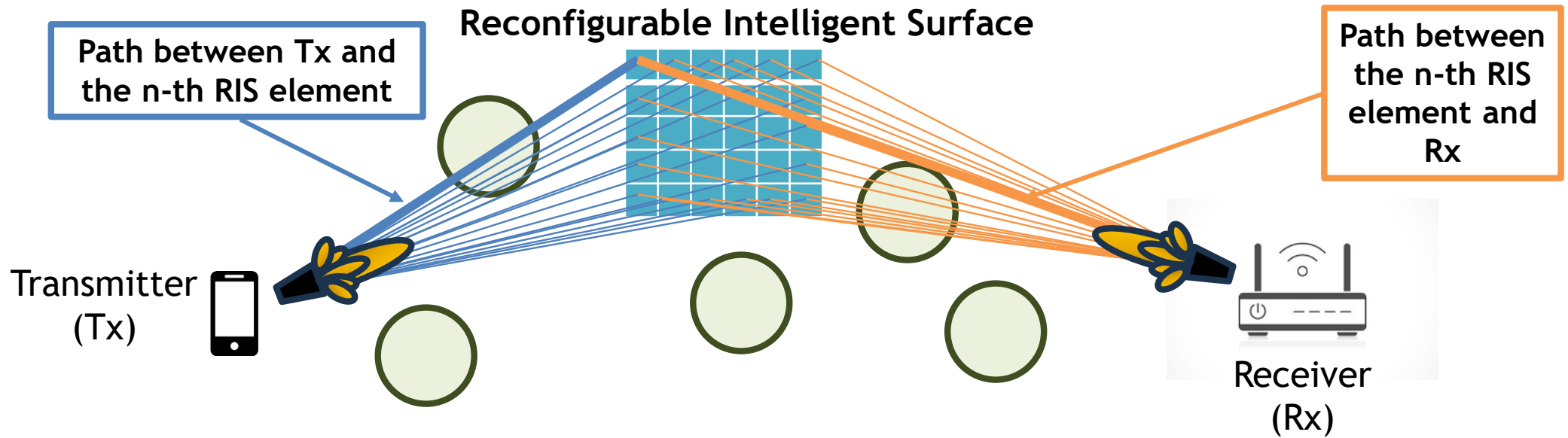
$$\mathcal{L}_{RIS} = 20 \log_{10} \left(\frac{4\pi}{\delta_x \delta_z} \right) - 10 \log_{10}(G_t G_r B) - 20 \log_{10} \left| \sum_{m=1}^M \sum_{n=1}^N \sqrt{\frac{F_{m,n}^{(eq)}}{D_{m,n}^{(eq)}} \frac{1}{r_{m,n}^t r_{m,n}^r}} \right|. \quad (2)$$

- Based on the Tang Path Loss Model [3]



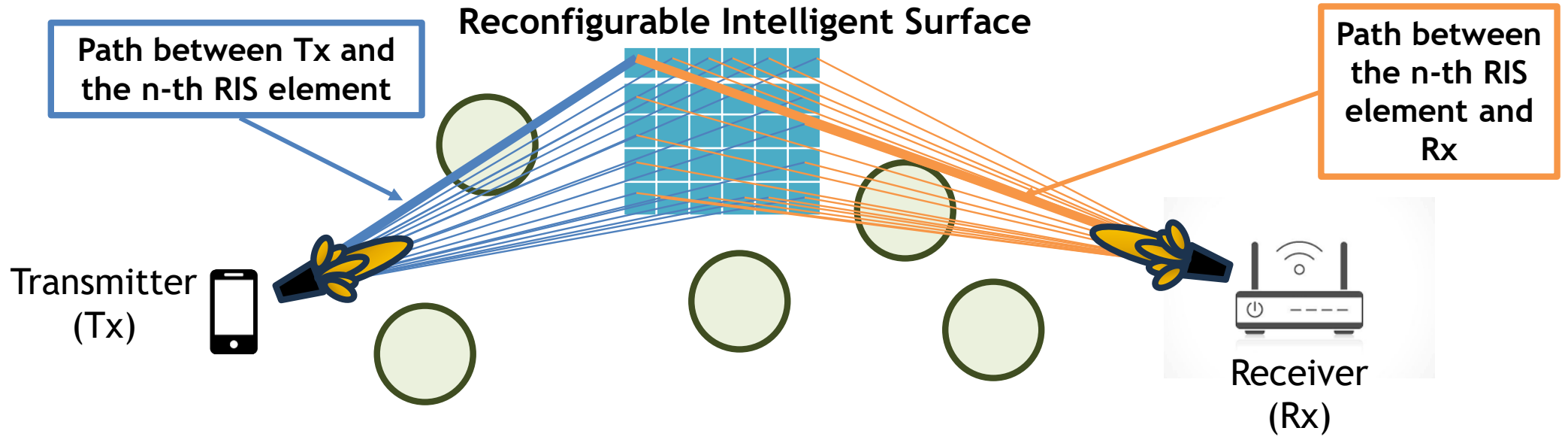
$$\mathcal{L}_{RIS} = 20 \log_{10} \left(\frac{4\pi}{\delta_x \delta_z} \right) - 10 \log_{10}(G_t G_r B) - 20 \log_{10} \left| \sum_{m=1}^M \sum_{n=1}^N \sqrt{\frac{F_{m,n}^{(eq)}}{D_{m,n}^{(eq)}}} \frac{1}{r_{m,n}^t r_{m,n}^r} \right|. \quad (2)$$

Free-Space Path Loss



$$\mathcal{L}_{RIS} = 20 \log_{10} \left(\frac{4\pi}{\delta_x \delta_z} \right) - 10 \log_{10}(G_t G_r B) - 20 \log_{10} \left| \sum_{m=1}^M \sum_{n=1}^N \sqrt{\frac{F_{m,n}^{(eq)}}{D_{m,n}^{(eq)}} \frac{1}{r_{m,n}^t r_{m,n}^r}} \right|. \quad (2)$$

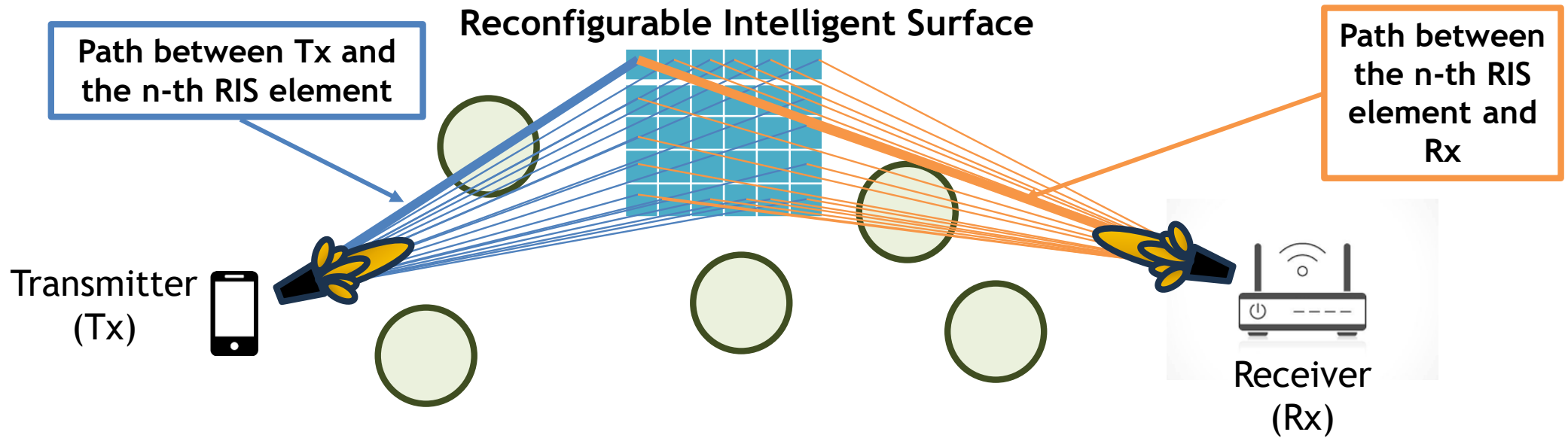
- Consider the contribution of each path Tx-(RIS element)-Rx.
- Subsequently, each the model combine the individual contributions.



$$\mathcal{L}_{RIS} = 20 \log_{10} \left(\frac{4\pi}{\delta_x \delta_z} \right) - 10 \log_{10}(G_t G_r B) - 20 \log_{10} \left| \sum_{m=1}^M \sum_{n=1}^N \sqrt{\frac{F_{m,n}^{(eq)}}{D_{m,n}^{(eq)}} \frac{1}{r_{m,n}^t r_{m,n}^r}} \right|. \quad (2)$$

- Each contribution includes the effects of the antennas' power radiation patterns.

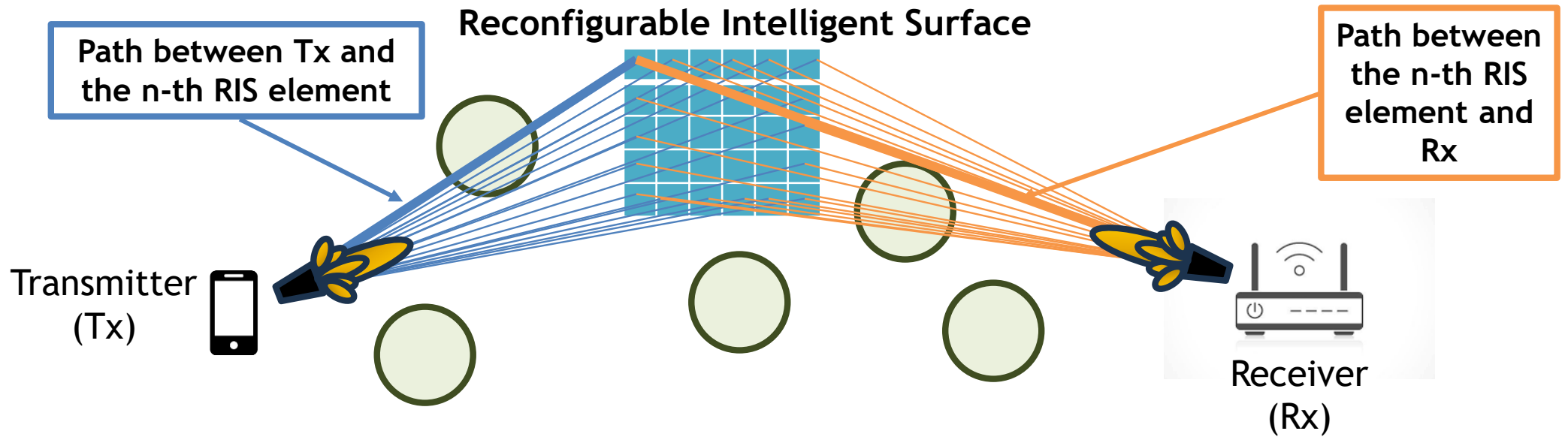
$$F_{m,n}^{(eq)} = F(\theta_{m,n}^t, \varphi_{m,n}^t) F(\theta_t^{m,n}, \varphi_t^{m,n}) F(\theta_r^{m,n}, \varphi_r^{m,n}) F(\theta_{m,n}^r, \varphi_{m,n}^r)$$



$$\mathcal{L}_{RIS} = 20 \log_{10} \left(\frac{4\pi}{\delta_x \delta_z} \right) - 10 \log_{10}(G_t G_r B) - 20 \log_{10} \left| \sum_{m=1}^M \sum_{n=1}^N \sqrt{\frac{F_{m,n}^{(eq)}}{D_{m,n}^{(eq)} r_{m,n}^t r_{m,n}^r}} \right|. \quad (2)$$

- Our model incorporates the effects of transmissions medium and attenuation due to obstructions on each path Tx-(RIS element)-Rx.

$$D_{m,n}^{(eq)} = 10^{\frac{A_0(r_{m,n}^t + r_{m,n}^r)}{10}} 10^{\frac{\zeta(X_{m,n}^t + X_{m,n}^r)}{10}}.$$

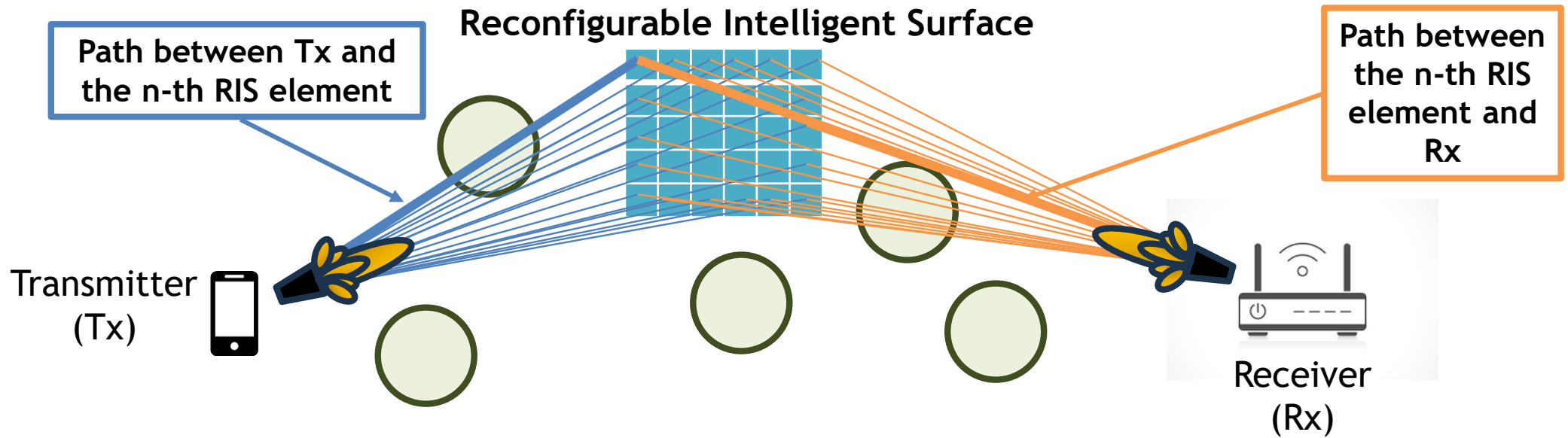


$$\mathcal{L}_{RIS} = 20 \log_{10} \left(\frac{4\pi}{\delta_x \delta_z} \right) - 10 \log_{10}(G_t G_r B) - 20 \log_{10} \left| \sum_{m=1}^M \sum_{n=1}^N \sqrt{\frac{F_{m,n}^{(eq)}}{D_{m,n}^{(eq)} r_{m,n}^t r_{m,n}^r}} \right|. \quad (2)$$

- Our model incorporates the effects of transmissions medium and attenuation due to obstructions on each path Tx-(RIS element)-Rx.

Attenuation due to
transmission medium
PATH LENGTH

$$D_{m,n}^{(eq)} = 10^{\frac{A_0(r_{m,n}^t + r_{m,n}^r)}{10}} 10^{\frac{\zeta(X_{m,n}^t + X_{m,n}^r)}{10}}.$$

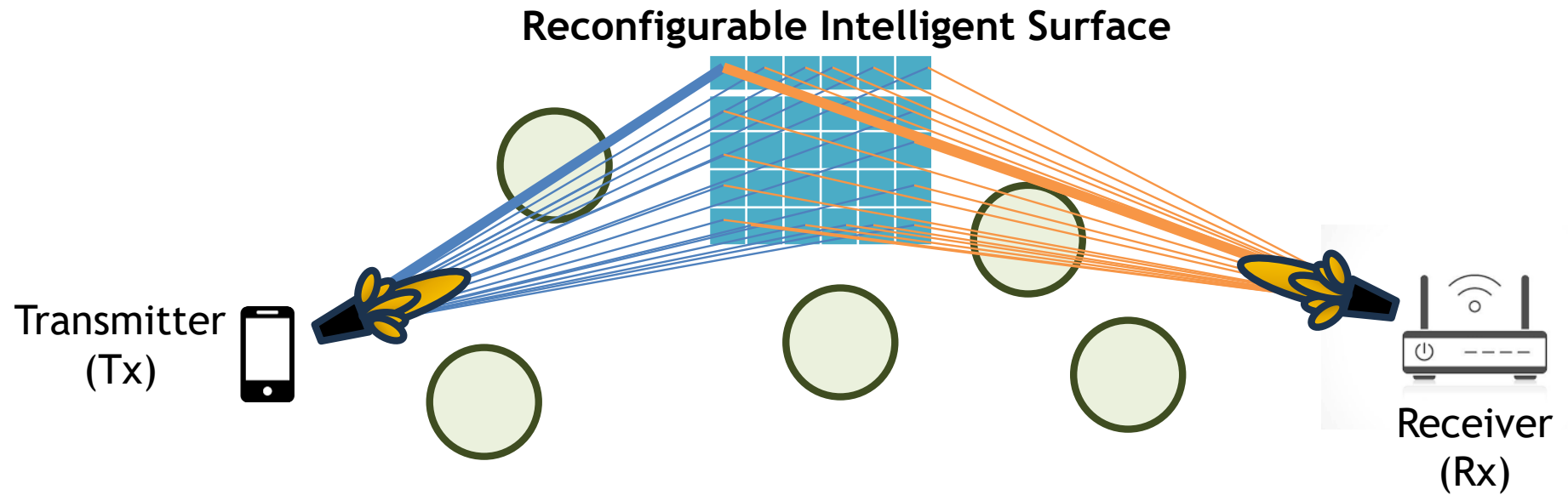


$$\mathcal{L}_{RIS} = 20 \log_{10} \left(\frac{4\pi}{\delta_x \delta_z} \right) - 10 \log_{10}(G_t G_r B) - 20 \log_{10} \left| \sum_{m=1}^M \sum_{n=1}^N \sqrt{\frac{F_{m,n}^{(eq)}}{D_{m,n}^{(eq)}}} \frac{1}{r_{m,n}^t r_{m,n}^r} \right|. \quad (2)$$

- Our model incorporates the effects of transmissions medium and attenuation due to obstructions on each path Tx-(RIS element)-Rx.

$$D_{m,n}^{(eq)} = 10^{\frac{A_0(r_{m,n}^t + r_{m,n}^r)}{10}} 10^{\frac{\zeta(X_{m,n}^t + X_{m,n}^r)}{10}}.$$

Attenuation due to obstructions
OBSTRUCTION LENGTH



$$\mathcal{L}_{RIS} = 20 \log_{10} \left(\frac{4\pi}{\delta_x \delta_z} \right) - 10 \log_{10}(G_t G_r B) - 20 \log_{10} \left| \sum_{m=1}^M \sum_{n=1}^N \sqrt{\frac{F_{m,n}^{(eq)}}{D_{m,n}^{(eq)}}} \frac{1}{r_{m,n}^t r_{m,n}^r} \right|. \quad (2)$$

- **Assumptions:**

- All RIS elements have the same amplitude response.
- Phase responses of RIS elements are adjusted to maximize power at the receiver.

SNR and Outage Probability

- Tx and Rx are aligned through **beamsteering**.
- The alignment is optimal in terms of **signal-to-noise ratio (SNR)**

$$\gamma_k = \frac{P_t |h|^2}{\sigma^2} 10^{-\frac{\mathcal{L}_k}{10}}.$$

← SNR of the k-th path

- The system selects the **least attenuated path**: between LOS path and RIS-path

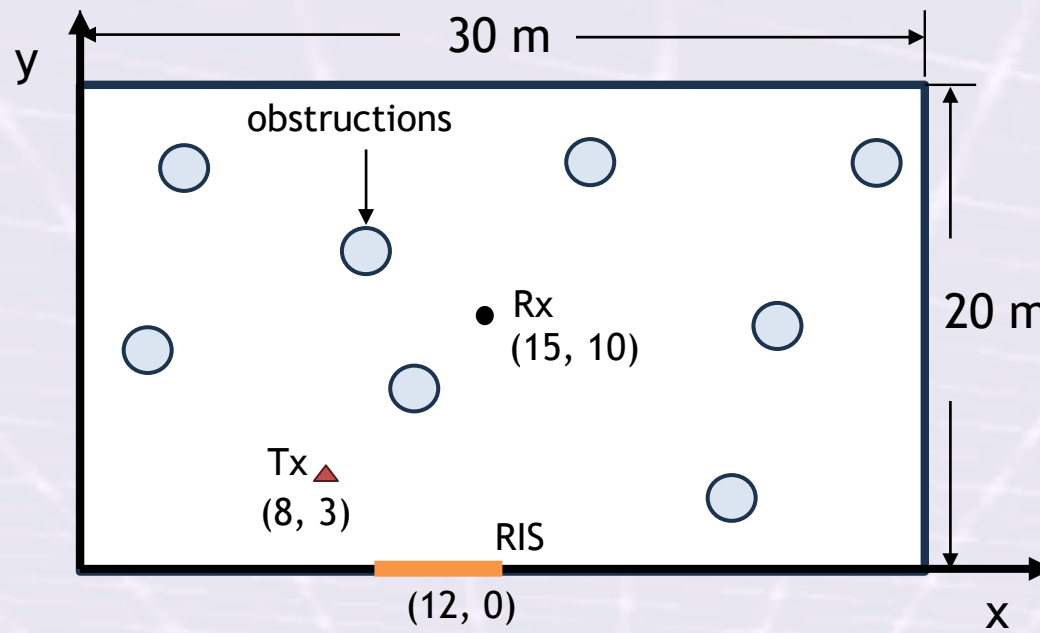
$$\gamma = \frac{P_t |h|^2}{\sigma^2 \Upsilon}, \quad \text{where} \quad \Upsilon = \min_k \left\{ 10^{\frac{\mathcal{L}_k}{10}} \right\}.$$

- **Probability of Outage:**
 - Key Performance Indicator (KPI)
 - Determine whether the SNR is less than a given threshold.

$$P_{\text{out}}(\gamma_{\text{th}}) = \Pr(\Upsilon \leq \gamma_{\text{th}}).$$

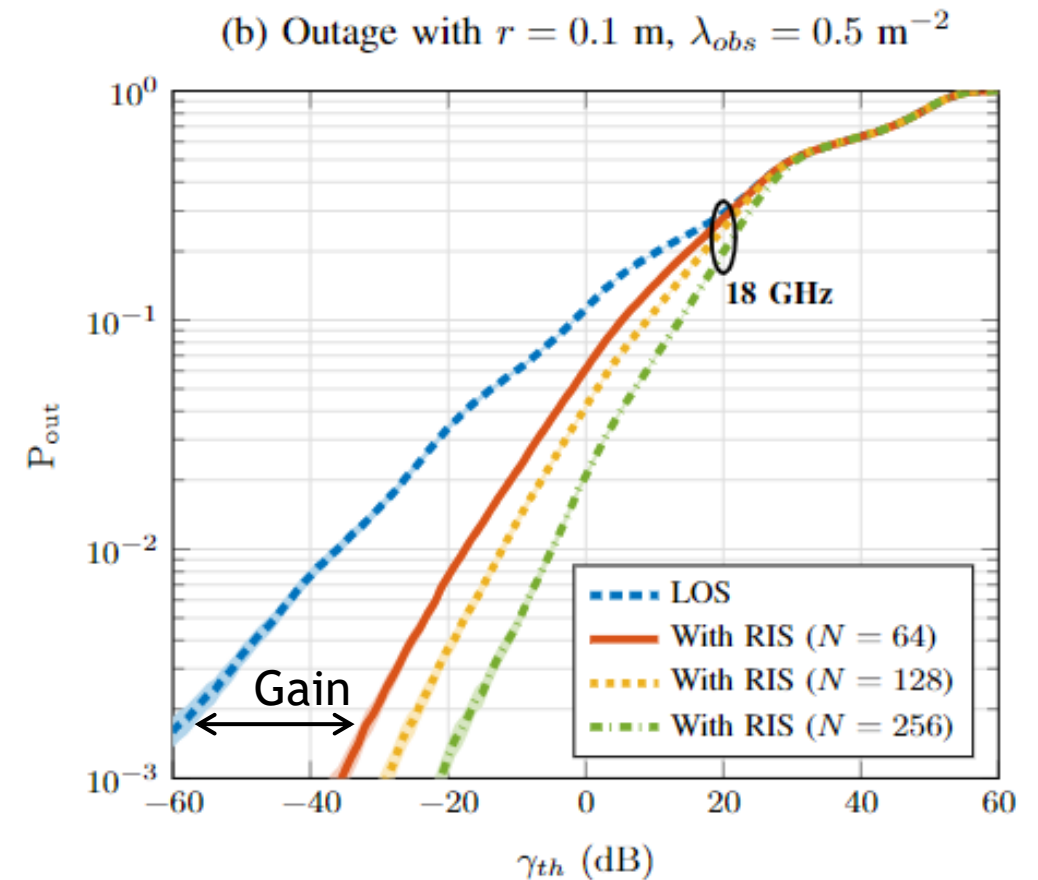
Numerical Simulations

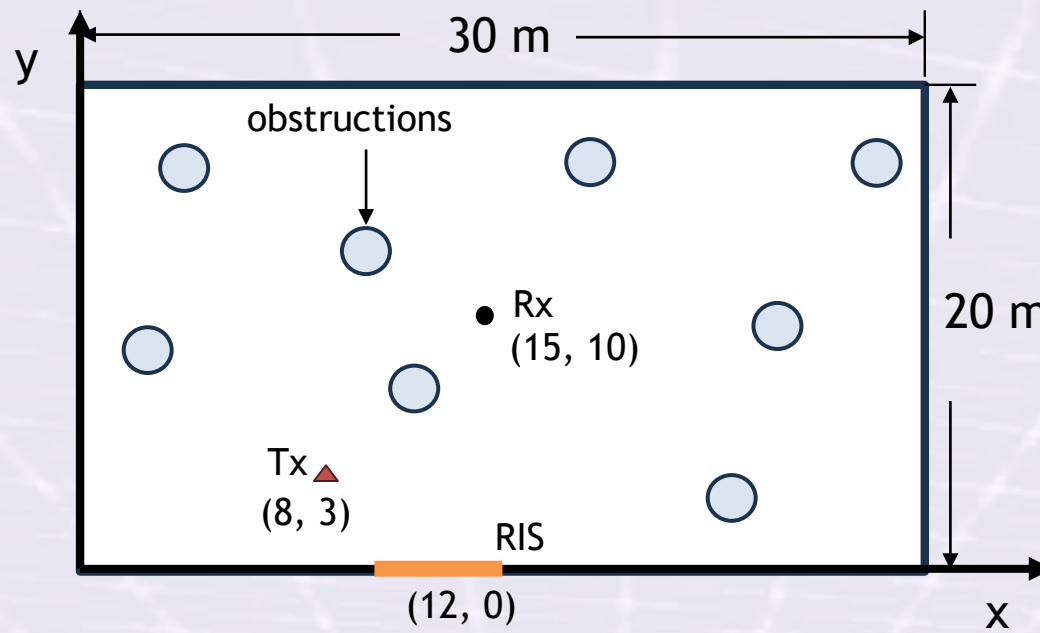
- **Objective:** Estimation of the outage probability in the presence of randomly located obstructions.
- **Path Loss Model:** considering
 - The effects of the transmission medium.
 - Attenuation of obstructing objects.
- Each data point is averaged over 100,000 realizations of the corresponding experiment.
- **Poisson Point Process (PPP):**
 - Each trial generates a different PPP with a specified density λ_{obs} to position object centers.
- **Obstruction shapes:**
 - **2D case:** circular obstructions.
 - **3D case:** spherical obstructions.



2D Indoor Case

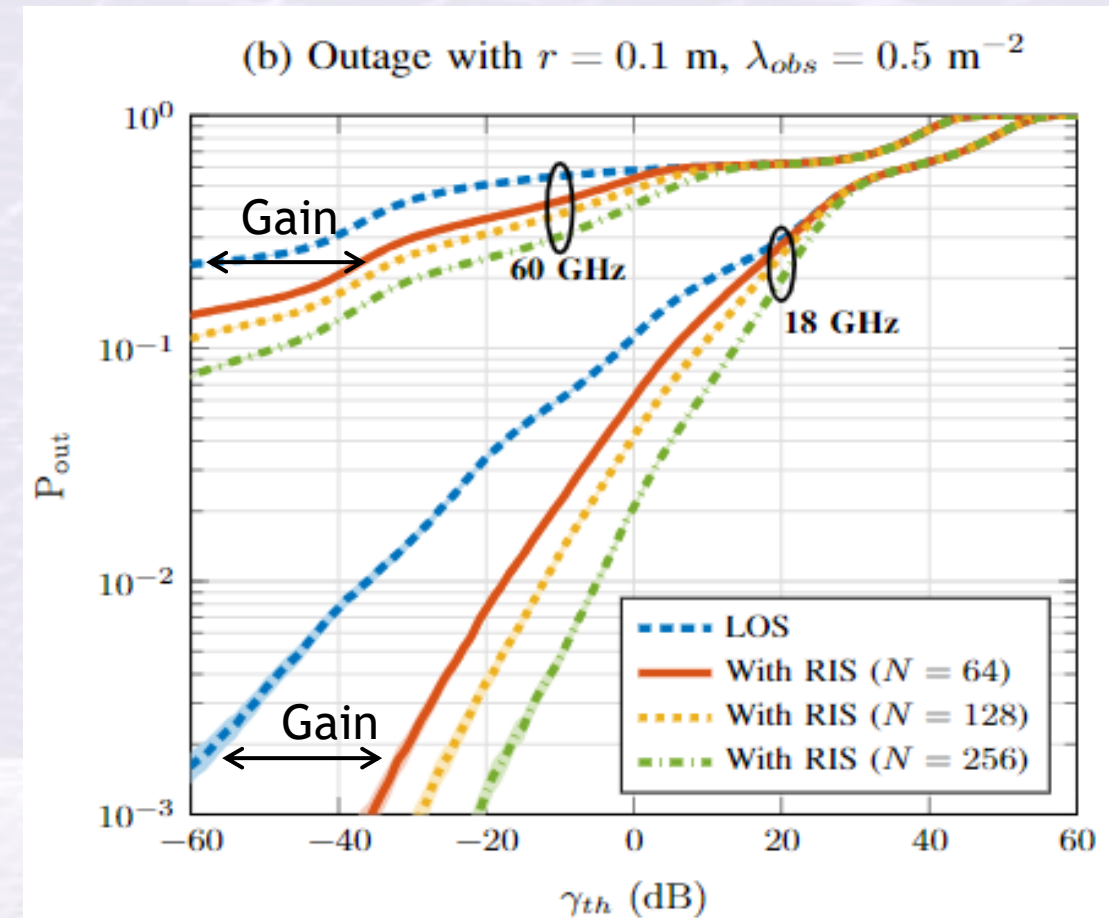
- Rectangular room: realistic environments
- Tx, Rx, and RIS are located in fixed positions
- Evaluate the performance of the RIS-aided system using different number of RIS elements.
- Circular obstructions



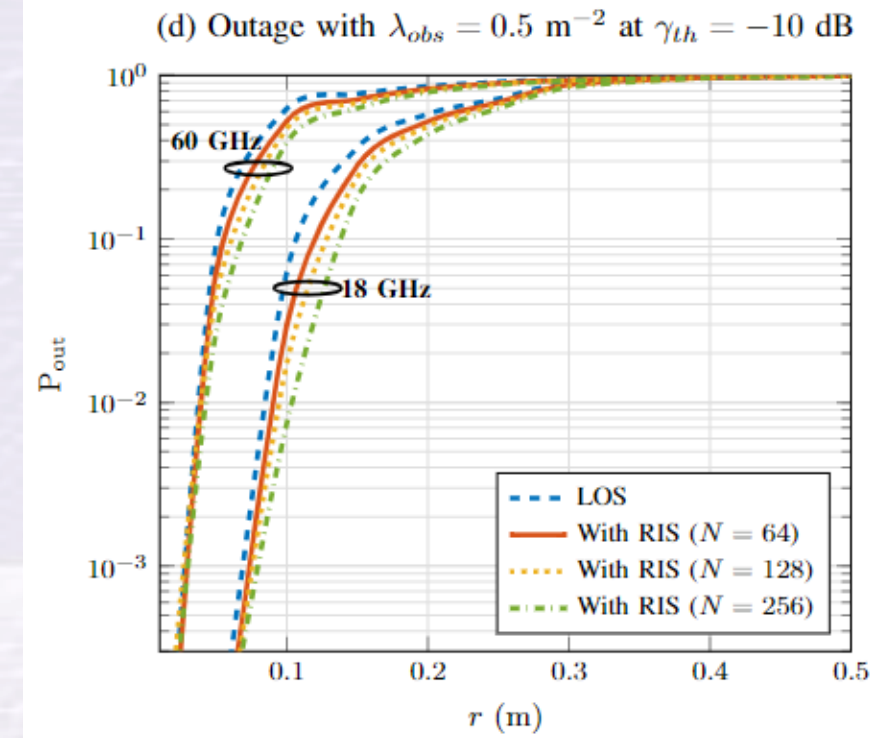
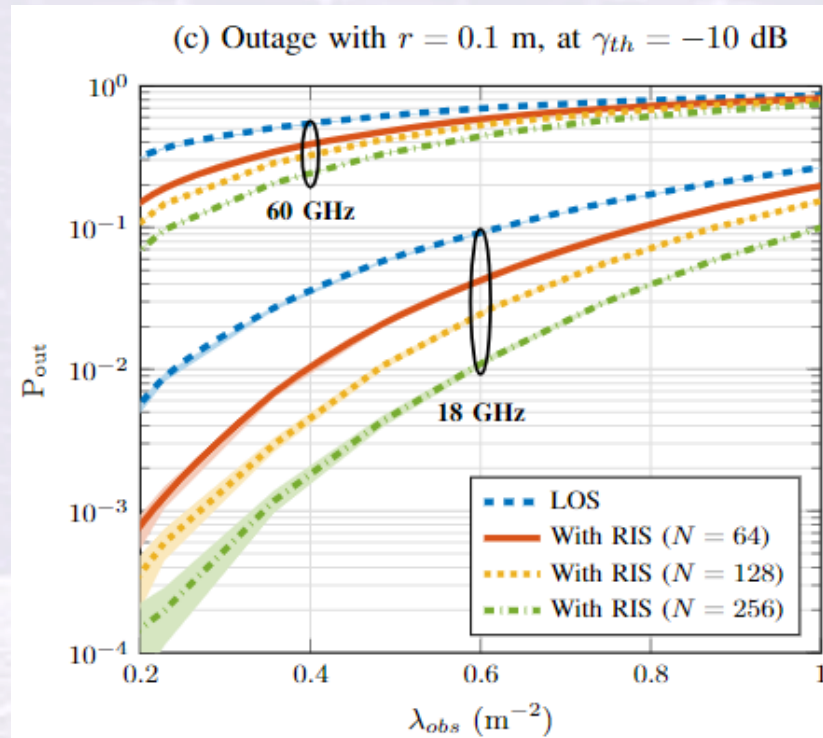
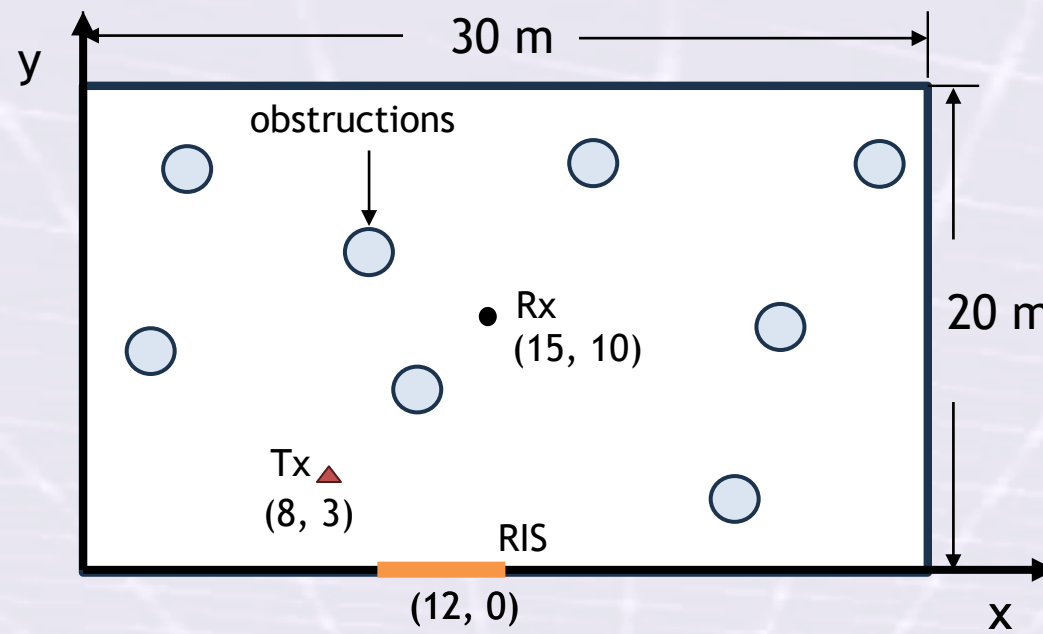


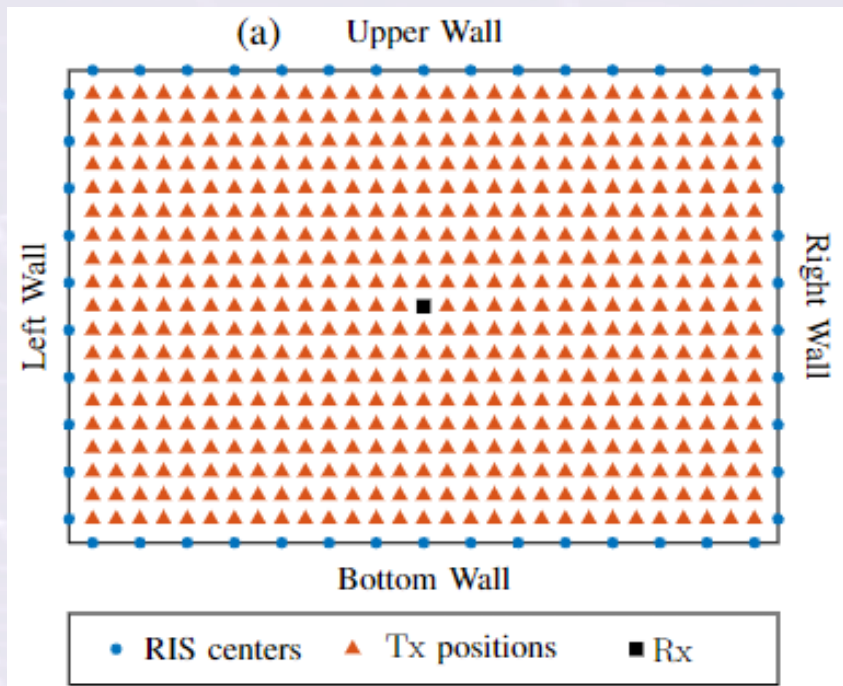
2D Indoor Case

- Rectangular room: realistic environments
- Tx, Rx, and RIS are located in fixed positions
- Evaluate the performance of the RIS-aided system using different number of RIS elements.
- Circular obstructions



2D Indoor Case



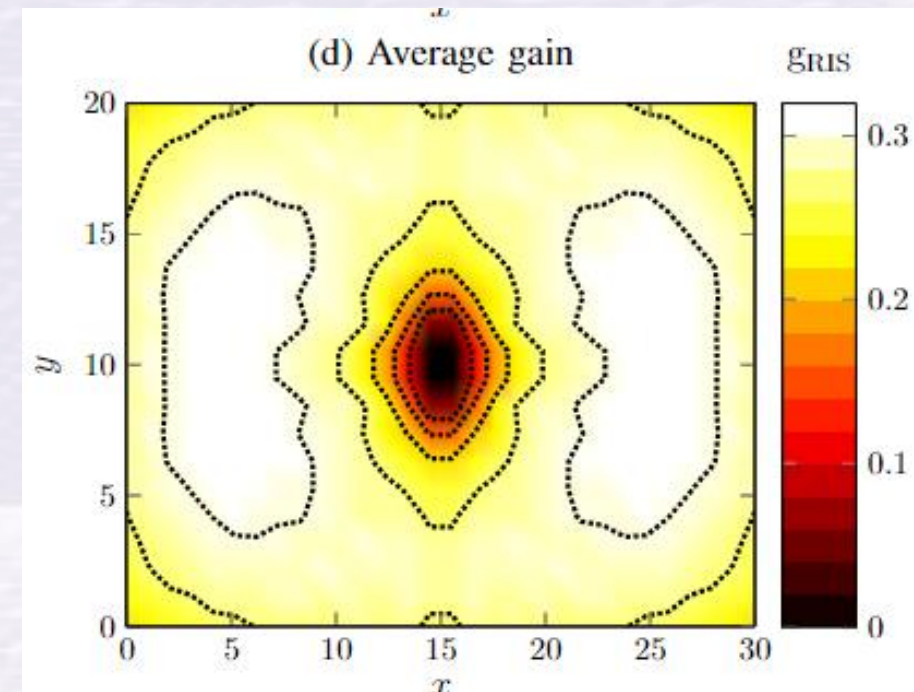
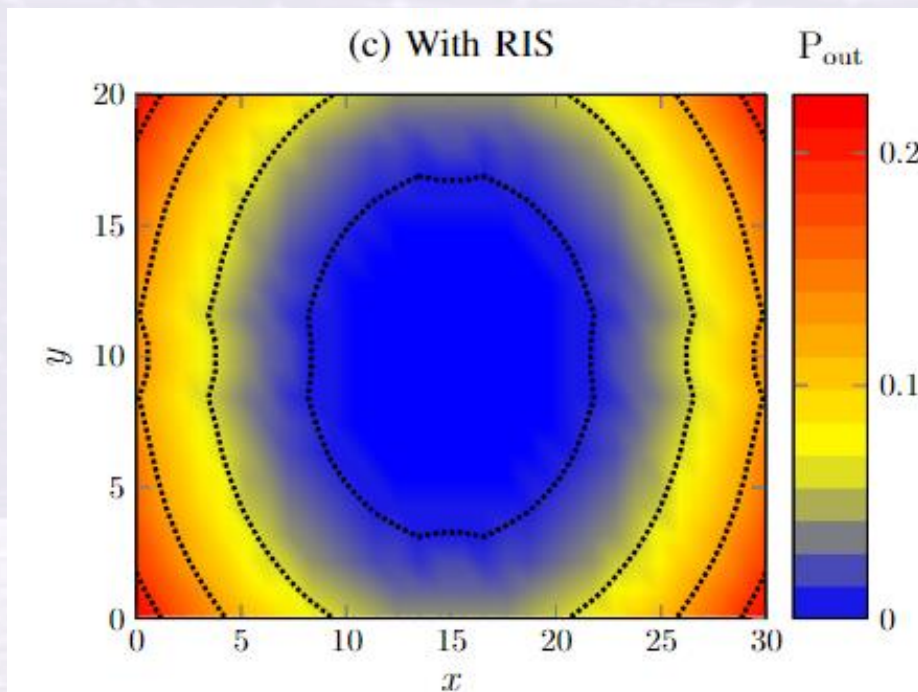


Multiple Tx positions

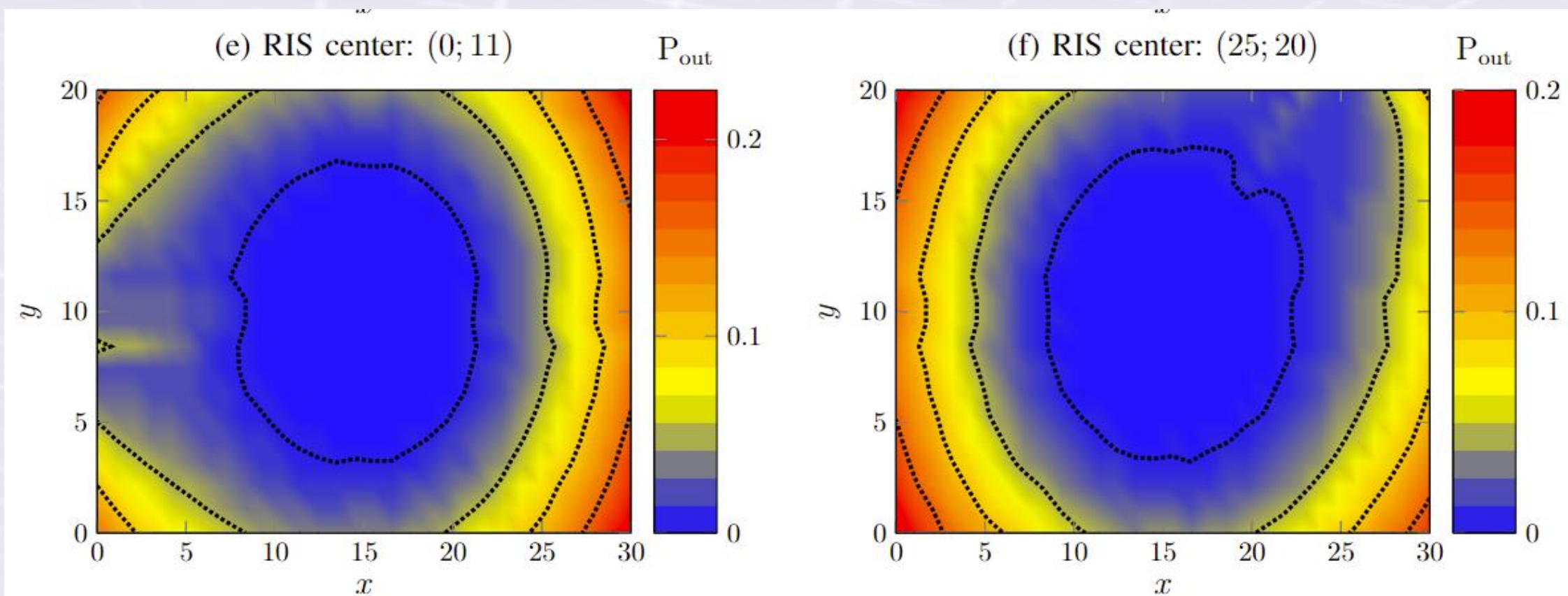
- Rx fixed position at (15, 10)
- Tx uniformly spaced horizontally and vertically

Relative Gain

$$g_{\text{RIS}} = \frac{P_{\text{out}}^{\text{[No RIS]}} - P_{\text{out}}^{\text{[With RIS]}}}{P_{\text{out}}^{\text{[No RIS]}}}$$



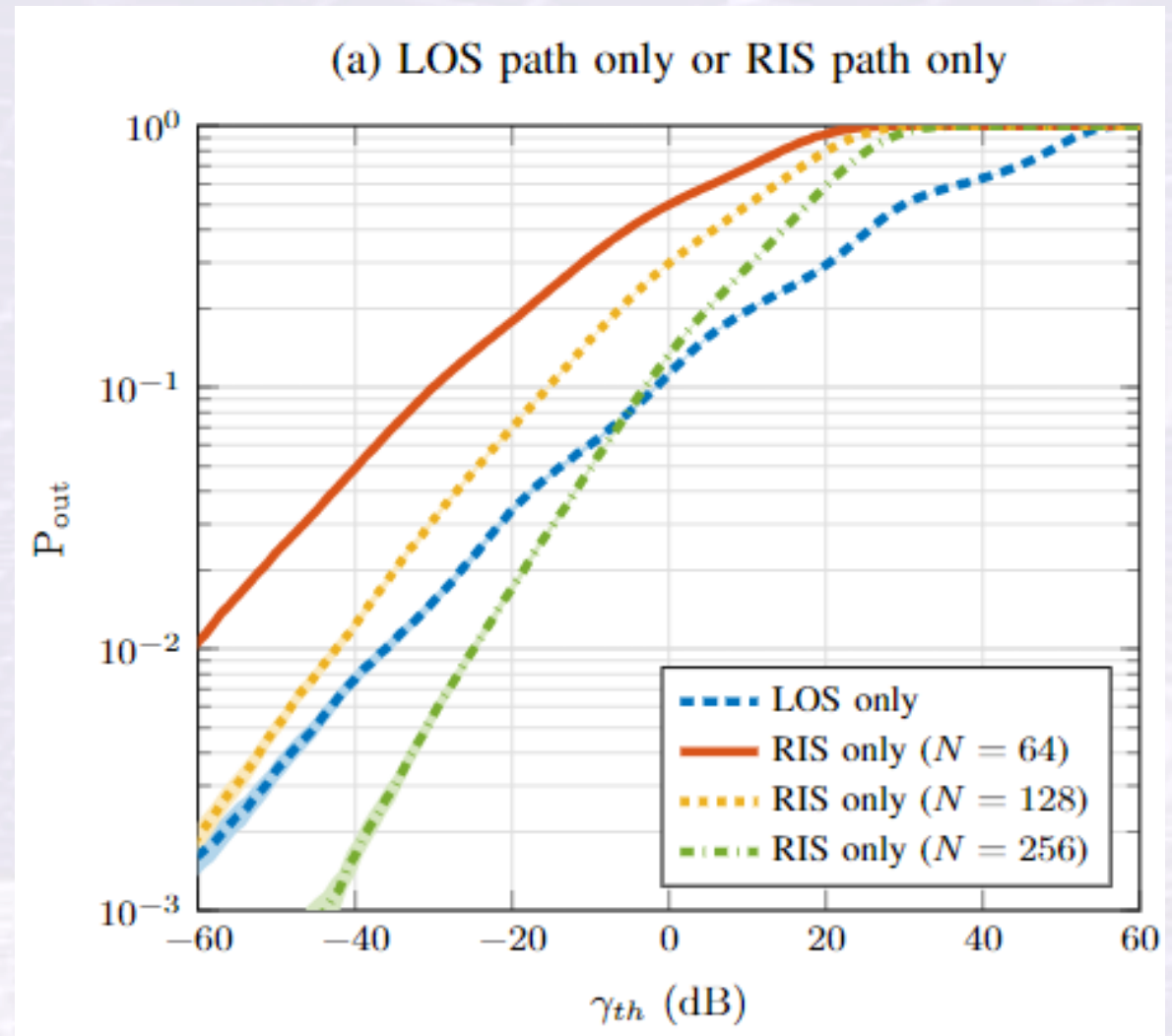
Multiple Tx positions



Absence of Beamsteering

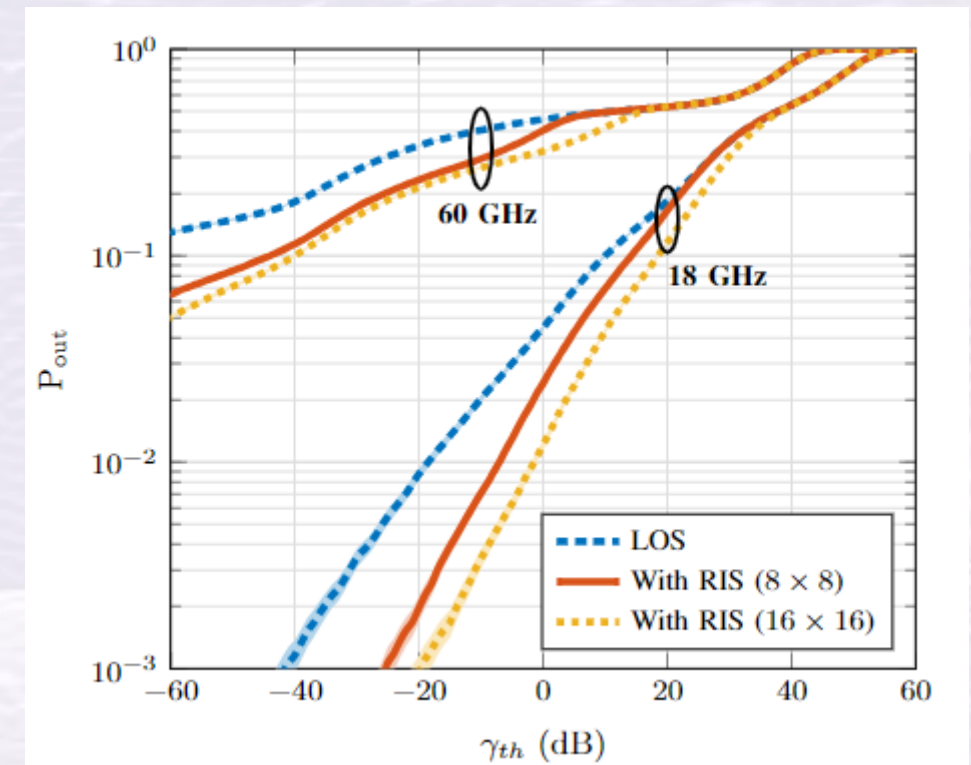
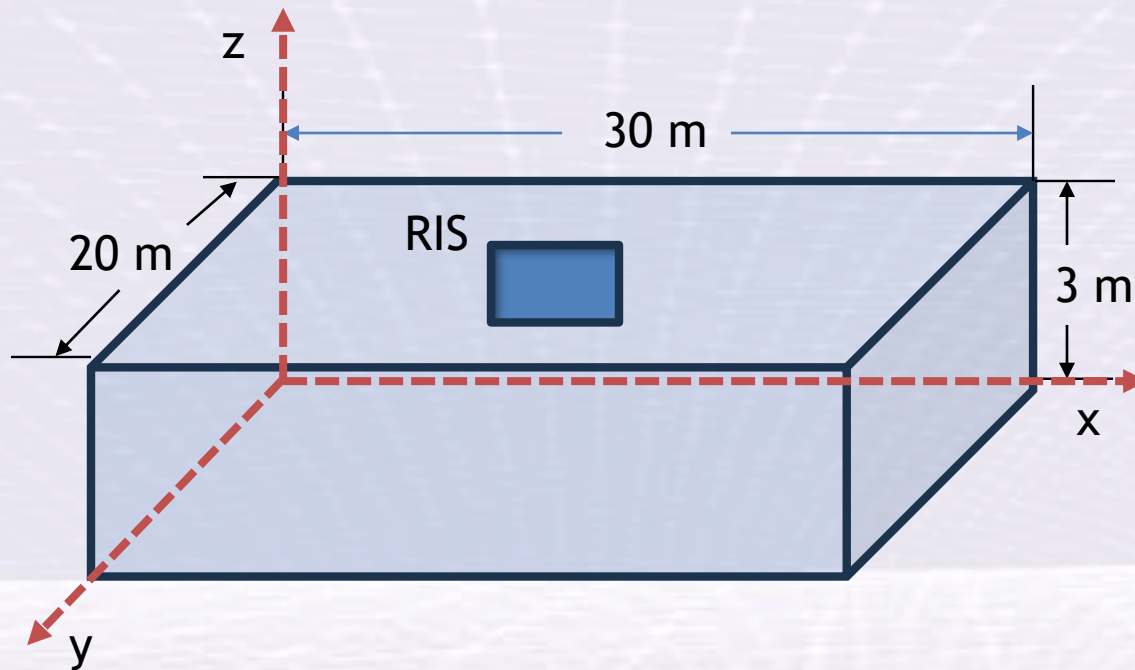
- **Objective:**

- Evaluate the quality of the RIS path relative to LOS path.
- Performance of the RIS path when the LOS path is blocked.



3D Indoor Case

- **Transmitter (Tx) position:** Coordinates (8, 3, 1)
- **Receiver (Rx) position:** Coordinates (15, 10, 2.5)
 - Located at the center of the room, just below the ceiling.
- **RIS center position:** Coordinates (12, 0, 1.5)



Conclusions and Future Work

- **A comprehensive path loss model of RIS-aided wireless communication system:**
 - Include the effects of the transmission medium.
 - Consider the attenuation of obstructing objects.
- **Outage Probability Estimation:**
 - Focused on indoor scenarios with randomly located obstructions.
 - RIS positioning and Transmitter locations.
 - Beamsteering scenarios.
 - A 3D indoor case.
- **Future work**
 - Develop and propose simplified models for RIS-aided systems.

Acknowledgments

This work has been supported by Project AEON-CPS (TSI-063000-2021-38), funded by the Ministry of Economic Affairs and Digital Transformation and the European Union NextGeneration-EU in the Spanish Recovery, Transformation, and Resilience Plan framework.



Questions?

- **Path loss model of RIS-assisted system:**

1. ELLINGSON, Steven W. Path loss in reconfigurable intelligent surface-enabled channels. En 2021 IEEE 32nd Annual International Symposium on Personal, Indoor and Mobile Radio Communications (PIMRC). IEEE, 2021. p. 829-835.
2. TANG, Wankai, et al. Wireless communications with reconfigurable intelligent surface: Path loss modeling and experimental measurement. IEEE transactions on wireless communications, 2020, vol. 20, no 1, p. 421-439.
3. TANG, Wankai, et al. Path loss modeling and measurements for reconfigurable intelligent surfaces in the millimeter-wave frequency band. IEEE Transactions on Communications, 2022, vol. 70, no 9, p. 6259-6276.
4. DI RENZO, Marco, et al. Analytical modeling of the path-loss for reconfigurable intelligent surfaces-anomalous mirror or scatterer?. En 2020 IEEE 21st International Workshop on Signal Processing Advances in Wireless Communications (SPAWC). IEEE, 2020. p. 1-5.
5. GRADONI, Gabriele; DI RENZO, Marco. End-to-end mutual coupling aware communication model for reconfigurable intelligent surfaces: An electromagnetic-compliant approach based on mutual impedances. IEEE Wireless Communications Letters, 2021, vol. 10, no 5, p. 938-942.
6. NAJAFI, Marzieh, et al. Physics-based modeling and scalable optimization of large intelligent reflecting surfaces. IEEE Transactions on Communications, 2020, vol. 69, no 4, p. 2673-2691.
7. HUANG, Jie, et al. Reconfigurable intelligent surfaces: Channel characterization and modeling. Proceedings of the IEEE, 2022, vol. 110, no 9, p. 1290-1311.
8. ABDELNABI, Amr A.; MANCUSO, Vincenzo; AJMONE MARSAN, Marco. Outage of millimeter wave links with randomly located obstructions. IEEE Access, 2020, vol. 8, p. 139404-139421.